

S.T. Yau High School Science Award (Asia)**2020****Research Report****The Team**

Registration Number: Chem-040

Name of team member: YU Xinjie

School: Hwa Chong Institution

City, Country: Singapore, Singapore

Name of supervising teacher: CHEN Zhengbo

Position: Associate Professor

School/Institution: Capital Normal University

City, Country: Beijing, China

Title of Research Report

Colorimetric discrimination of multiple antioxidants based on three chloroauric acid/core-shell Au@Ag nanocube sensors

Date

31/08/2020

Colorimetric discrimination of multiple antioxidants based on three chloroauric acid/core-shell Au@Ag nanocube sensors

YU Xinjie

Abstract

Antioxidant species are crucial to normal biological functions, yet inappropriate doses of certain species have deleterious effects on human health. In this study, a colorimetric sensor array for the discrimination of multiple antioxidants has been developed. In order to extract data-rich colorimetric responses from the sensor array, Au@Ag nanocubes (NCs) with a core-shell structure as colorimetric probes were rationally prepared, and three different concentrations of chloroaurate acid (HAuCl_4) were employed as sensing elements. Interestingly, Au^{3+} ions can be reduced to different valence states (i.e., Au(0) and Au(I)) by different antioxidants, thus effectively inhibited the oxidation etching process of Au@Ag NCs by Au(III) ions to varying extents, generating simultaneous colorimetric signal output to enable identification of the six antioxidants at 10 nM via linear discriminant analysis (LDA). The discrimination ability of the sensor array was further evaluated in antioxidant mixtures from binary to component mixture. Remarkably, identification of these six antioxidants spiked in urine was also realized with 100% of accuracy.

Keywords: Au@Ag nanocubes, sensor array, silver etching, antioxidant, linear discriminant analysis

Acknowledgement

I would like to express my gratitude to my mentor, Dr. Chen Zhengbo for his guidance and support, without which this research project would not be possible.

2020 S.-T. Yau High School Science Award

Commitments on Academic Honesty and Integrity

We hereby declare that we

1. are fully committed to the principle of honesty, integrity and fair play throughout the competition.
2. actually perform the research work ourselves and thus truly understand the content of the work.
3. observe the common standard of academic integrity adopted by most journals and degree theses.
4. have declared all the assistance and contribution we have received from any personnel, agency, institution, etc. for the research work.
5. undertake to avoid getting in touch with assessment panel members in a way that may lead to direct or indirect conflict of interest.
6. undertake to avoid any interaction with assessment panel members that would undermine the neutrality of the panel member and fairness of the assessment process.
7. observe all rules and regulations of the competition.
8. agree that the decision of YHSA(Asia) is final in all matters related to the competition.

We understand and agree that failure to honour the above commitments may lead to disqualification from the competition and/or removal of reward, if applicable; that any unethical deeds, if found, will be disclosed to the school principal of team member(s) and relevant parties if deemed necessary; and that the decision of YHSA(Asia) is final and no appeal will be accepted.

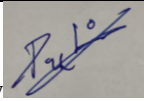
(Signatures of full team below)

郁

Name of team member: Yu Xinjie

陈, 郑博

Name of supervising teacher: Chen Zhengbo

Noted and endorsed by 

PHEE-TAN Peh Ling

Table of Contents

1. Introduction.....	5
2. Experiment Section.....	8
2.1 Chemicals.....	8
2.2 Apparatus.....	8
2.3 Preparation of Au@Ag NCs.....	8
2.4 Discrimination procedure of different antioxidants.....	9
3. Results and discussion.....	10
3.1 Discrimination principle.....	10
3.2 Characterization of the Au@Ag NCs.....	11
3.2 Optimization of sensing conditions.....	12
3.3 Array's discrimination performance.....	13
3.4 Discrimination of mixtures of antioxidants.....	15
3.5 Assay specificity.....	16
3.6 Application to real urine samples.....	16
4. Conclusion.....	17
Bibliography.....	18
Appendix.....	18

1. Introduction

In normal cellular metabolism, reactive oxidative species (ROS) are often produced. However, excess ROS lead to oxidative stress in biological systems. Under high oxidative stress, biomolecules vital to cellular processes undergo structural or functional changes, ultimately resulting in tissue damage¹. Consumption of antioxidants has been shown to help restore the biochemical balance between ROS and cellular antioxidative activity. Specific antioxidants, in due amounts, are able to prevent complex diseases including diabetes, stroke, Parkinson's disease, cardiovascular disorders, inflammatory diseases, and cancer². For instance, dopamine (DA) has been shown to resist shock. Citric acid (CA) can reduce the risk of cardiovascular arteriosclerosis by regulating blood viscosity. Inappropriate use of other antioxidants, however, is demonstrated to cause cancer and even life loss^{3,4}. Hence, it is desirable to develop a reliable and versatile method for determination and discrimination of antioxidants.

While there has not been a standardised method to determine antioxidant capacity, current *in-vitro* methods can be classified into two broad categories consisting of single electron transfer (ET)-based assays and hydrogen atom transfer (HAT)-based assays⁵. Common ET-based assays include the Folin-

¹ Laguerre, M.; Decker, E. A.; Lecomte, J.; Villeneuve, P. Methods for Evaluating the Potency and Efficacy of Antioxidants. *Curr. Opin. Clin. Nutr. Metab. Care* 2010, 13, 518-525.

² Barberis, A.; Spissu, Y.; Bazzu, G.; Fadda, A.; Azara, E.; Sanna, D.; Schirra, M.; Serra, P. A. Development and Characterization of an Ascorbate Oxidase-Based Sensor-Biosensor System for Telemetric Detection of AA and Antioxidant Capacity in Fresh Orange Juice. *Anal. Chem.* 2014, 86, 8727-8734.

³ Botterweck, A. A. M.; Verhagen, H.; Goldbohm, R. A.; Kleinjans, J.; van den Brandt, P. A. Intake of Butylated Hydroxyanisole and Butylated Hydroxytoluene and Stomach Cancer Risk: Results from Analyses in the Netherlands Cohort Study. *Food Chem. Toxicol.* 2000, 38, 599-605.

⁴ Li, H.; Lin, H.; Wang, X.; Lv, W.; Li, F. Dopamine-Based Paper Analytical Device for Truly Equipment-Free and Naked-Eye Biosensing Based on the Target-Initiated Catalyzed Oxidation. *ACS Appl. Mater. Interfaces* 2019, 11, 36469-36475.

⁵ Piyanan, T., Athipornchai, A., Henry, C. S., & Sameenoi, Y. (2018). An Instrument-free Detection of Antioxidant Activity Using Paper-based Analytical Devices Coated with Nanoceria. *Analytical Sciences*, 34(1), 97-102. doi:10.2116/analsci.34.97

Ciocalteu reagent^{6,7}, Ferric reducing-antioxidant power^{8,9} (FRAP), Cupric ion reducing antioxidant capacity¹⁰ (CUPRAC), 2,2-diphenyl-1-picrylhydrazyl¹¹ (DPPH), and ABTS/trolox equivalent antioxidant capacity¹² (TEAC). Common HAT-based assays include oxygen radical absorbance capacity^{13,14,15,16} (ORAC) and total radical trapping antioxidant parameter¹⁷ (TRAP). All of these methods require large reagent and sample volumes, and thus require cumbersome, labour intensive

⁶ Prior, R. L., Wu, X., & Schaich, K. (2005). Standardized Methods for the Determination of Antioxidant Capacity and Phenolics in Foods and Dietary Supplements. *Journal of Agricultural and Food Chemistry*, 53(10), 4290-4302. doi:10.1021/jf0502698

⁷ Alcalde, B., Granados, M., & Saurina, J. (2019). Exploring the Antioxidant Features of Polyphenols by Spectroscopic and Electrochemical Methods. *Antioxidants*, 8(11), 523. doi:10.3390/antiox8110523

⁸ Aaby, K., Hvattum, E., & Skrede, G. (2004). Analysis of Flavonoids and Other Phenolic Compounds Using High-Performance Liquid Chromatography with Coulometric Array Detection: Relationship to Antioxidant Activity. *Journal of Agricultural and Food Chemistry*, 52(15), 4595-4603. doi:10.1021/jf0352879

⁹ Bean, H., Radu, F., De, E., Schuler, C., Leggett, R. E., & Levin, R. M. (2008). Comparative evaluation of antioxidant reactivity within obstructed and control rabbit urinary bladder tissue using FRAP and CUPRAC assays. *Molecular and Cellular Biochemistry*, 323(1-2), 139-142. doi:10.1007/s11010-008-9972-5

¹⁰ Özyürek, M., Güçlü, K., Tütem, E., Başkan, K. S., Erçağ, E., Çelik, S. E., . . . Apak, R. (2011). A comprehensive review of CUPRAC methodology. *Analytical Methods*, 3(11), 2439. doi:10.1039/c1ay05320e

¹¹ Baiano, A., Terracone, C., Gambacorta, G., & Notte, E. L. (2009). Phenolic Content and Antioxidant Activity of Primitivo Wine: Comparison among Winemaking Technologies. *Journal of Food Science*, 74(3). doi:10.1111/j.1750-3841.2009.01101.x

¹² Huang, D., Ou, B., & Prior, R. L. (2005). The Chemistry behind Antioxidant Capacity Assays. *Journal of Agricultural and Food Chemistry*, 53(6), 1841-1856. doi:10.1021/jf030723c

¹³ Leeuw, R. V., Kevers, C., Pincemail, J., Defraigne, J., & Dommès, J. (2014). Antioxidant capacity and phenolic composition of red wines from various grape varieties: Specificity of Pinot Noir. *Journal of Food Composition and Analysis*, 36(1-2), 40-50. doi:10.1016/j.jfca.2014.07.001

¹⁴ Rivero-Pérez, M. D., González-Sanjosé, M. L., Ortega-Herás, M., & Muñoz, P. (2008). Antioxidant potential of single-variety red wines aged in the barrel and in the bottle. *Food Chemistry*, 111(4), 957-964. doi:10.1016/j.foodchem.2008.05.013

¹⁵ Prior, R. L., Wu, X., & Schaich, K. (2005). Standardized Methods for the Determination of Antioxidant Capacity and Phenolics in Foods and Dietary Supplements. *Journal of Agricultural and Food Chemistry*, 53(10), 4290-4302. doi:10.1021/jf0502698

¹⁶ Aaby, K., Hvattum, E., & Skrede, G. (2004). Analysis of Flavonoids and Other Phenolic Compounds Using High-Performance Liquid Chromatography with Coulometric Array Detection: Relationship to Antioxidant Activity. *Journal of Agricultural and Food Chemistry*, 52(15), 4595-4603. doi:10.1021/jf0352879

¹⁷ Canabady-Rochelle, L. L., Harscoat-Schiavo, C., Kessler, V., Aymes, A., Fournier, F., & Girardet, J. (2015). Determination of reducing power and metal chelating ability of antioxidant peptides: Revisited methods. *Food Chemistry*, 183, 129-135. doi:10.1016/j.foodchem.2015.02.147

sample preparation and handling. It should be emphasized that these methods are difficult to achieve high-throughput screening of multiple antioxidants.

Colorimetric assays provide new opportunities for distinguishing and determining antioxidant species due to its simplicity and practicality. Such methods do not require sophisticated equipment and produce results observable by the naked eye. Various colorimetric methods based on etching and subsequent aggregation of nanoparticles (NPs) have emerged. However, NP-based methods often suffer from poor specificity due to the similar oxidation susceptibility among antioxidants¹⁸. An improved assay would retain the ease of operation and also exhibit high degree of specificity. The array sensing technique proves such improvement possible. Rather than the conventional “lock-key” interaction between sensor-target couples¹⁹, drawing inspiration from the mechanisms of mammalian olfactory/gustatory responses²⁰, sensor arrays generate multiple responses based on the cross-responsiveness of a series of receptors to a particular target.

In this study, we report a novel colorimetric sensor array for discrimination of six types of antioxidants (i.e., citric acid (CA), tartaric acid (TA), ascorbic acid (AA), tea polyphenol (TP), tannic acid (TA), and gallic acid (GA)). In this design, three concentrations of H₂AuCl₄ were employed as sensor receptors, and core-shell Au@Ag nanocubes (NCs) served as colorimetric probes. As we know, Ag shell is etched by Au³⁺ and induces a colour change. However, the presence of various antioxidants inhibits the oxidation activity of Au³⁺ to different extents. Consequently, the Au@Ag NCs are etched to diverse degrees upon the introduction of different antioxidants due to the reaction between antioxidant and Au³⁺ and exhibit differential colorimetric responses. The response pattern as a fingerprint is unique to each analyte and can be identified by linear discriminant analysis (LDA).

¹⁸ Huang, W., Seehafer, K., & Bunz, U. H. (2019). Discrimination of Flavonoids by a Hypothesis Free Sensor Array. *ACS Applied Polymer Materials*, 1(6), 1301-1307. doi:10.1021/acsapm.9b00116

¹⁹ Ko, J.; Bhagwat, N.; Yee, S. S.; Ortiz, N.; Sahnoud, A.; Black, T.; Aiello, N. M.; McKenzie, L.; O'Hara, M.; Redlinger, C.; Romeo, J.; Carpenter, E. L.; Stanger, B. Z.; Issadore, D. Combining Machine Learning and Nanofluidic Technology To Diagnose Pancreatic Cancer Using Exosomes. *ACS Nano* 2017, 11, 11182–11193.

²⁰ You, C. C.; Miranda, O. R.; Gider, B.; Ghosh, P. S.; Kim, I. B.; Erdogan, B.; Krovi, S. A.; Bunz, U. H. F.; Rotello, V. M. Detection and Identification of Proteins Using Nanoparticle-Fluorescent Polymer ‘Chemical Nose’ Sensors. *Nat. Nanotechnol.* 2007, 2, 318–323.

2. Experiment Section

2.1 Chemicals

HAuCl₄, AgNO₃, NaBH₄, ascorbic acid (AA), cetyltrimethylammonium bromide (CTAB), and cetyltrimethylammonium chloride (CTAC) were obtained from Sigma-Aldrich. Citric acid (CA), tartaric acid (TA), ascorbic acid (AA), tea polyphenol (TP), tannic acid (TA), and gallic acid (GA) were purchased from Aladdin (Shanghai, China). Ultrapure water (18.2 MΩ/cm) was acquired from a Milli-Q ultrapure system. All the reagents were analytical grade.

2.2 Apparatus

Absorption values were recorded on SpectraMax^{RM2e} Multi-Mode Microplate Reader (Molecular Devices, California, USA). Transmission electron microscopy (TEM) images were performed on a JEM-2100 microscope at an acceleration voltage of 200 kV (JEOL, Japan). The absorption of the 96-well plate at 425 nm was collected by a SpectraMax M2e microplate reader (Molecular Devices, U.S.A.).

2.3 Preparation of Au@Ag NCs

The preparation process of Au@Ag NCs can be found in previous literature²¹. The synthesis is divided into three steps: the first step is to synthesize Au seeds, the second step is to synthesize CTAC-capped Au seeds, and the third step is to synthesize Au@Ag NCs. The whole preparation process is as follows: We first mixed 5 mL of 0.25 mM HAuCl₄ and 5 mL of 100 mM CTAB. 0.6 mL of 10 mM ice cooled NaBH₄ was then added into the solution. The yellow solution turned colourless upon addition. An eventual light red colouration was obtained after 3 h, indicating the formation of 3 nm Au seeds.

²¹ Ma, Y. Y.; Li, W. Y.; Cho, E. C.; Li, Z. Y.; Yu, T.; Zeng, J.; Xie, Z. X.; Xia, Y. N. Au@Ag Core-Shell Nanocubes with Finely Tuned and Well-Controlled Sizes, Shell Thicknesses, and Optical Properties. *ACS Nano*. 2010, 4, 675-6734. DOI: 10.1021/nn102237c

The complete dissolution of NaBH_4 was ensured by keeping the 3 nm Au seed solution at room temperature for 3 h. Subsequently, 4.5 mL of 100 mM AA was added to 12 mL of the mixture composed of 6 mL of 0.5 mM HAuCl_4 and 6 mL of 0.2 M CTAC, followed by the addition of 0.3 mL of 3 nm Au seeds. A colour change from colourless to claret was observed. After resting 1 h, the suspension of Au nanocrystals was centrifuged at 15000 rpm for 30 min. Then the Au nanocrystals were washed thoroughly with water and dispersed in deionized water. Next, 0.5 mL of the previous CTAC-Au seeds and 4.5 mL of 20 mM CTAC were mixed. The mixture was heated at 60 °C for 20 min under magnetic stirring. 2 mL of 2 mM AgNO_3 and a mixture of 1 mL of 50 mM AA and 1 mL of 40 mM CTAC were simultaneously added using a syringe pump. The colour changed from red to brown. Stirring was continued at 60 °C for 4 h and the resulting mixture was cooled in an ice-bath. Finally, the product was separated by centrifugation at 15000 rpm for 15 min. The resulting Au@Ag NCs were washed with deionized water three times and stored at 4 °C before use.

2.4 Discrimination procedure of different antioxidants

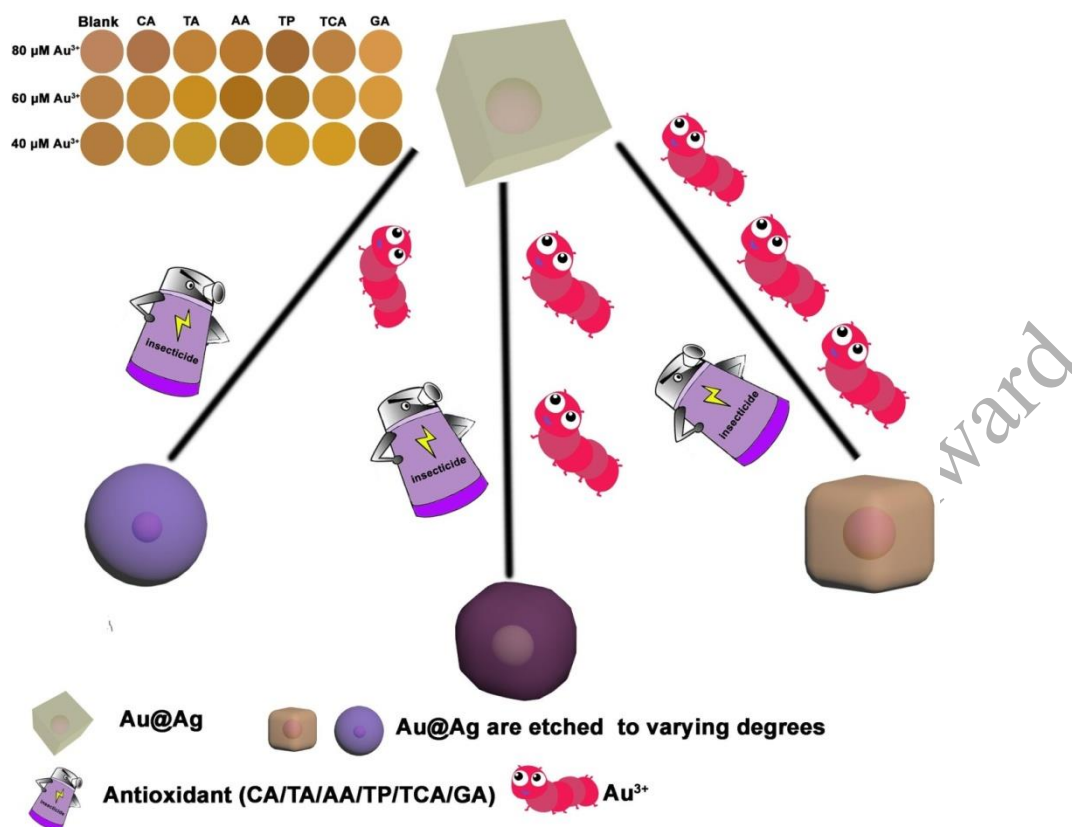
Firstly, 100 μL of three concentrations (40, 60, and 80 μM) of HAuCl_4 and 370 μL of Au@Ag NC solution were well mixed in phosphate buffered saline (PBS) (pH=7.0) to form three $\text{HAuCl}_4/\text{Au@Ag}$ NCs sensors (40 μM $\text{HAuCl}_4/\text{Au@Ag}$ NCs, 60 μM $\text{HAuCl}_4/\text{Au@Ag}$ NCs, and 80 μM $\text{HAuCl}_4/\text{Au@Ag}$ NCs). Then, 100 μL of target antioxidants (CA, TA, AA, TP, TA, and GA) were individually injected to the above sensor solutions for 30 min of incubation. Next, 100 μL of the above solutions were transferred into 96-well plates, and then the absorption of each well at 425 nm was measured by a microplate reader. Therefore, the six antioxidants were measured against the three $\text{HAuCl}_4/\text{Au@Ag}$ NCs sensors 5 times to give a training data matrix of 6 antioxidants \times 3 sensors \times 5 replicates.

3. Results and discussion

3.1 Discrimination principle

The sensing strategy of the method is presented in Scheme 1, three sensing elements (40, 60, and 80 μM HAuCl_4) are first formed to fabricate the sensor array. In the absence of target antioxidants, galvanic exchange occurs between Au@Ag NCs and Au(III), Ag of the Au@Ag NCs is etched, meanwhile, Au(III) ions are reduced to Au(0) and deposited onto the surface of Au@Ag NCs, generating changes of colour and absorbance intensity. Whereas in the presence of different antioxidants, Au(III) can be reduced to other valence states, such as its zero and mono valence state, which effectively inhibits the oxidation etching process of Au@Ag NCs to varying degrees. Consequently, diverse colour and absorbance changes as “fingerprint” can be observed after the addition of antioxidants, and these gathered colorimetric signals from the sensor array can offer a map of a discriminative fingerprint by linear discriminant analysis (LDA)²². Therefore, an effective discrimination of the six antioxidants (i.e., CA, TA, AA, TP, TCA, and GA) can be achieved.

²² Jurs, P. C., Bakken, G. A., & McClelland, H. E. (2000). Computational Methods for the Analysis of Chemical Sensor Array Data from Volatile Analytes. *Chemical Reviews*, 100(7), 2649-2678. doi:10.1021/cr9800964



Scheme 1 Schematic illustration of the colorimetric discrimination of multiple antioxidants based on the etching of the Au@Ag NCs

3.2 Characterization of the Au@Ag NCs

The prepared Au@Ag NCs in the experiments were characterized by transmission electron microscopy (TEM) images. As shown in Fig. 1A, From the figure, we can clearly see that the nanoparticles have an obvious core-shell structure. HRTEM results (inset of Fig. 1A) verifies that the outer shell of the nanoparticle is Ag. The resulting elemental map ((inset of Fig. 1A) of the nanoparticles reveal that Au element was concentrated at the centre of the structure as the “core” and Ag element is distributed in the periphery of the structure as the “shell”. In addition, in the presence of antioxidants, as shown in Fig. 1(B,C), Au@Ag NCs were etched by Au^{3+} to different degrees, which is attributed to the inhibitory effect of different antioxidants on Ag etching.

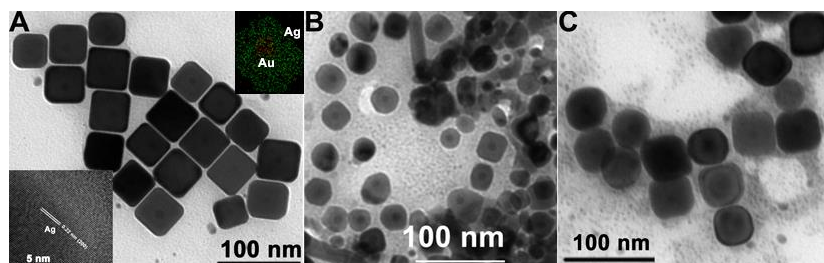


Figure 1 TEM image of Au@Ag NCs. Inset: HRTEM and element mapping. (B,C) TEM images of Au@Ag NCs after etching in the presence of different antioxidants.

3.2 Optimization of sensing conditions

To improve the effectiveness of the sensor array, several key parameters including pH and Au^{3+} concentration were optimised. The effect of solution pH on the absorbance was first investigated. As shown in Fig.S1, as the pH value varies in the range between 6.0 and 8, the absorption peak at 425 nm decreases. When pH=7.2, the absorbance at 425 nm decreases dramatically with the appearance of the peak at 450 nm. In consideration of the inhibitory effect of antioxidant (here AA) on Au@Ag NC etching, we chose 7.0 as the optimum pH. HAuCl_4 concentration, as array's sensing element, has a great influence on the performance of the sensor array. We investigated the effect of 8 HAuCl_4 concentrations (10, 20, 40, 60, 80, 100, 150, and 200 μM) on the absorbance of the solution. As depicted in Fig. S2, about 40, 60, and 80 μM HAuCl_4 , in which the absorption peaks at three different wavelengths appear, corresponding to different colours. Because the sensor array must consider differences in the recognition ability of sensing elements, we chose 40, 60, and 80 μM HAuCl_4 as the optimal concentrations of HAuCl_4 .

3.3 Array's discrimination performance

To test the discrimination ability of the sensor array, sensing behaviours of the sensor array to six antioxidants were conducted. In order to better illustrate the colorimetric responses of the sensor array, absorbance change ($\Delta A = A_{i,425\text{ nm}} - A_{0,425\text{ nm}}$) of each antioxidant was recorded, where A_i and A_0 represented the absorbance values of the Au@Ag NCs at 425 nm in the presence and absence of the targets, respectively. Each test was repeated five times. As shown in Fig.2, the colour map, acting as "fingerprints", clearly shows diverse changes between 6 antioxidants at the same concentration (10 nM), revealing the feasibility for antioxidant discrimination by the sensor array. To further investigate the colorimetric responses of the sensor array, linear discriminant analysis (LDA) was performed on the training matrices. The matrices were transformed into canonical factors and visualised in a three-dimensional (3D) diagram. As depicted in Fig. 3(A₁-F₁), the six antioxidants at each concentration (200, 150, 100, 50 20, and 10 nM) were located in six separate positions without any overlap. The discrete distribution of the six groups in the 3D LDA plot demonstrates that these six antioxidants could be well distinguished. In order to reveal the interaction pattern of each sensing elements and the target antioxidants, a "radar" pattern for the six antioxidants with the same concentration by the sensor array were formed as shown in Fig. 3(A₂-F₂), it clearly shows that a discernible discrepancy exists between the interaction patterns of each sensing elements and each antioxidants with the same concentration, like the colour map, further confirming the feasibility for antioxidant discrimination by the sensor array.

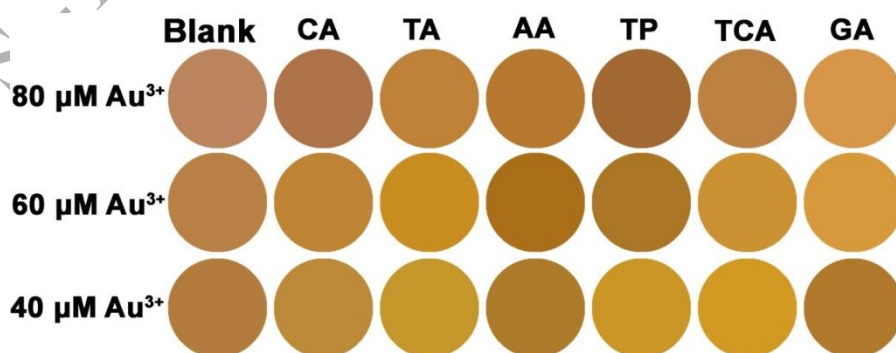
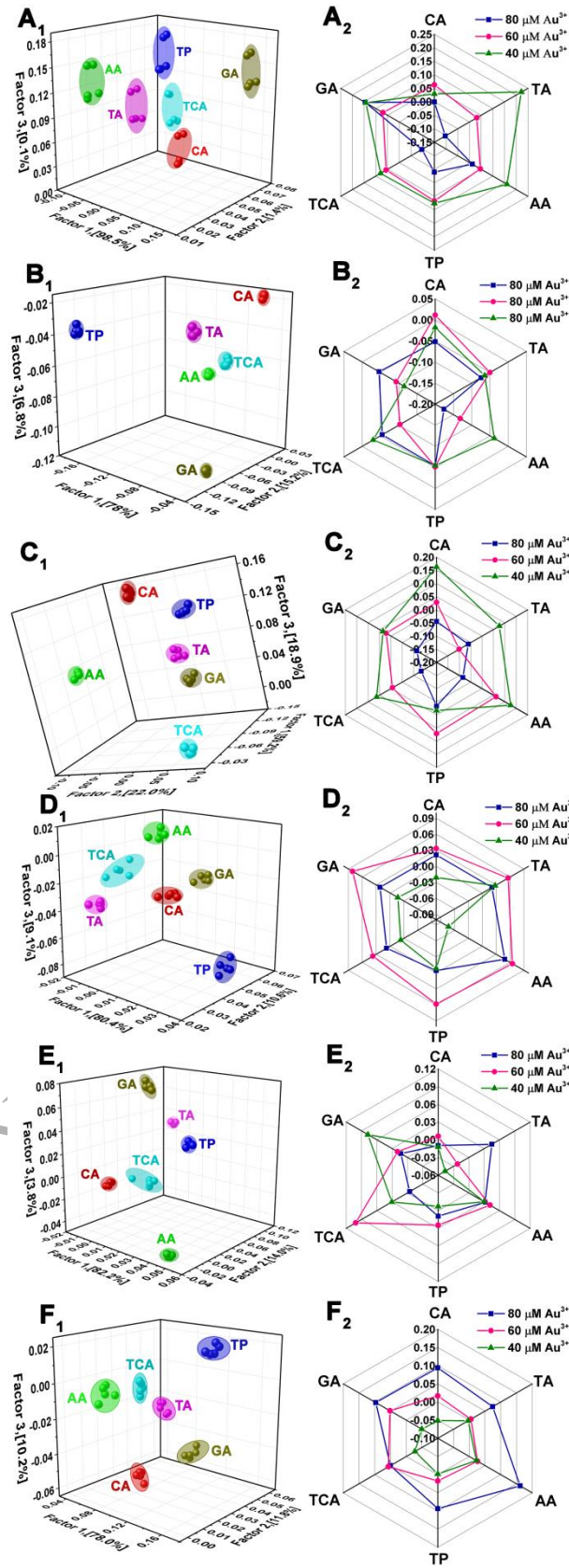


Figure 2 Photographs of Au@Ag NCs-based sensor array in the absence and presence of different antioxidants (all at 10 nM).



2020 S.T. Yau High School Science Award

Figure 3 (A₁-F₁) Canonical score plots, and (A₂-F₂) radar plots derived from absorbance changes of the sensor array toward the six different antioxidants at (A₁,A₂) 200 nM, (B₁,B₂) 150 nM, (C₁,C₂) 100 nM, (D₁,D₂) 50 nM, (E₁,E₂) 20 nM, and (F₁,F₂) 10 nM.

3.4 Discrimination of mixtures of antioxidants

As far as we know, it has been a great challenge for sensor arrays to differentiate antioxidant mixtures with different molar ratios. We prepared different molar ratios (CA:TA=4:6, CA:TA:GA=4:3:3, AA:TP:TCA=3:3:4, CA:AA:TP:TCA=1:2:3:4, CA:TA:TP:TCA:GA=2:1:2:3, and CA:TA:AA:TP:TCA:GA=2:2:1:2:1:2, with 100 nM total antioxidant) of mixtures and discriminated them by the sensor array. As depicted in Fig. 4, these mixtures with different molar ratios were well-clustered into six clusters and separated from each other, clearly demonstrating the sensor array also possesses discriminative capacity for mixtures of antioxidants of different compositions.

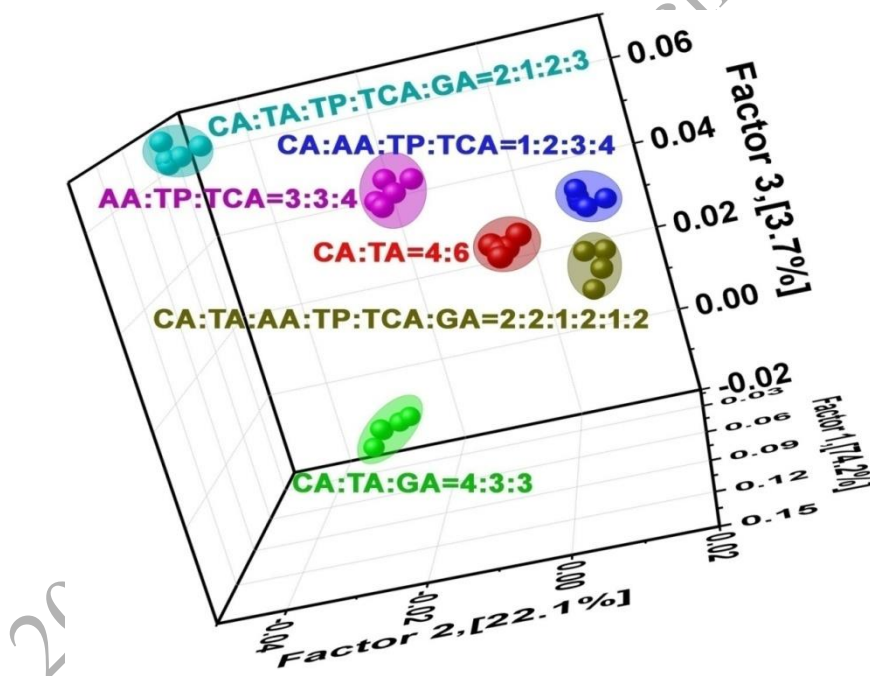


Figure 4 Canonical score plot for the colorimetric response patterns obtained against different molar ratios of the mixture of antioxidants.

3.5 Assay specificity

To assess the specificity of the as-fabricated assay, we selected three kinds of substances such as glutathione (GSH), histidine (His), and lysine (Lys) as interfering materials and investigated the effect of these species on the sensor array. As shown in Fig. 5A, although these interfering substances, each at 1 μ M, also produced obvious colorimetric responses, these responses were clearly distinct from those generated from the six target antioxidants at 100 nM. The result of the LDA analysis (Fig. 5B) satisfyingly reveals that the six target antioxidants can be discriminated effectively, and not any overlap occurs between the target antioxidants and the interfering substances. This result substantially suggested that the sensor array possessed a high degree of target specificity.

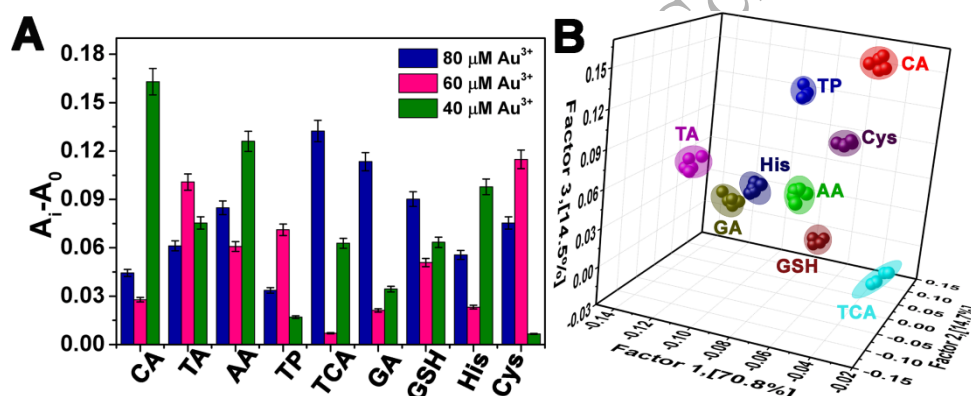


Figure 5 (A) Colorimetric response patterns (fingerprints) and (B) LDA score plots of the sensor array for identification of the six antioxidants (all at 100 nM) and the interfering species (all at 1 μ M).

3.6 Application to real urine samples

To further assess the practicability of the sensor array, we investigated whether the sensor array can identify the six antioxidants in human urine sources. We spiked the urine samples collected from our laboratory staff with different antioxidants to obtain 20 nM of samples. The obtained absorbance data matrices were analysed by LDA and HCA. As shown in Fig. 6, it was found that there is not any

connection or overlapping for the seven clusters (urine itself and six antioxidants). These results demonstrate the potential applications of the developed sensor array for effective discrimination of multiple antioxidants in real urine samples.

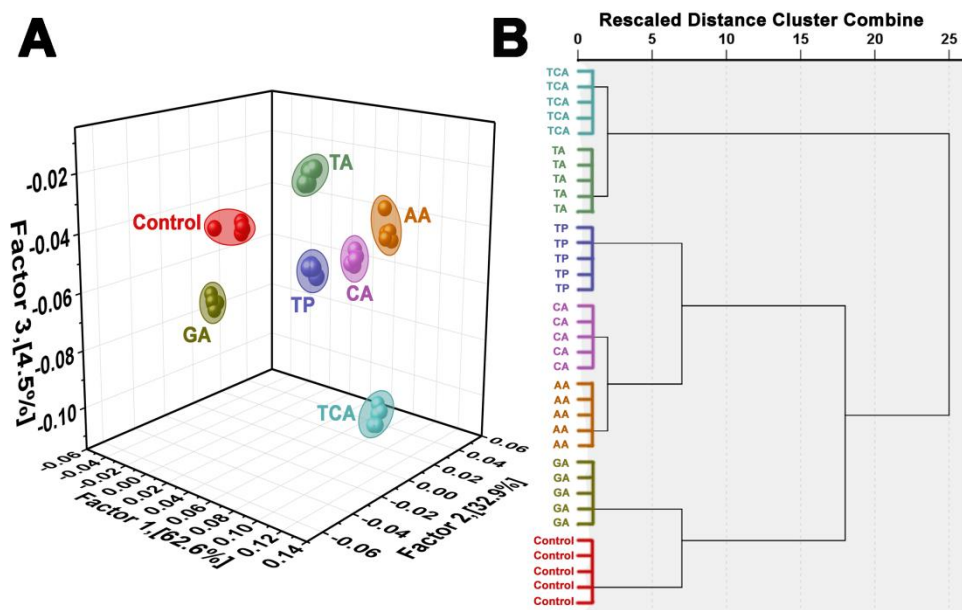


Figure 6.(A) Canonical score plot, and (B) HCA plot for the colorimetric response patterns obtained against 20 nM antioxidants in real urine samples.

4. Conclusion

In summary, a simple colorimetric sensor array consisting of three easy-to-prepare receptor units (40 μM Au^{3+} -Au@Ag NCs, 60 μM Au^{3+} -Au@Ag NCs, and 80 μM Au^{3+} -Au@Ag NCs) for discrimination of antioxidant species was developed. The sensor array shows that the differential interaction of target antioxidants with the sensing elements can inhibit the etching of Au@Ag NCs in varying degrees, which provided a characteristic fingerprint of the antioxidants. The sensor array demonstrated excellent ability to distinguish six antioxidants over a wide range of concentrations (10-200 nM) with 100% efficiency. Delightedly, the sensor array showed great anti-interferences and feasible potential for biofluids.

Bibliography

Aaby, K., Hvattum, E., & Skrede, G. (2004). Analysis of Flavonoids and Other Phenolic Compounds Using High-Performance Liquid Chromatography with Coulometric Array Detection: Relationship to Antioxidant Activity. *Journal of Agricultural and Food Chemistry*, 52(15), 4595-4603. doi:10.1021/jf0352879

Alcalde, B., Granados, M., & Saurina, J. (2019). Exploring the Antioxidant Features of Polyphenols by Spectroscopic and Electrochemical Methods. *Antioxidants*, 8(11), 523. doi:10.3390/antiox8110523

Baiano, A., Terracone, C., Gambacorta, G., & Notte, E. L. (2009). Phenolic Content and Antioxidant Activity of Primitivo Wine: Comparison among Winemaking Technologies. *Journal of Food Science*, 74(3). doi:10.1111/j.1750-3841.2009.01101.x

Barberis, A., Spissu, Y., Bazzu, G., Fadda, A., Azara, E., Sanna, D., . . . Serra, P. A. (2014). Development and Characterization of an Ascorbate Oxidase-based Sensor-Biosensor System for Telemetric Detection of AA and Antioxidant Capacity in Fresh Orange Juice. *Analytical Chemistry*, 86(17), 8727-8734. doi:10.1021/ac502066a

Barzilai, A., & Yamamoto, K. (2004). DNA damage responses to oxidative stress. *DNA Repair*, 3(8-9), 1109-1115. doi:10.1016/j.dnarep.2004.03.002

Bean, H., Radu, F., De, E., Schuler, C., Leggett, R. E., & Levin, R. M. (2008). Comparative evaluation of antioxidant reactivity within obstructed and control rabbit urinary bladder tissue using FRAP and CUPRAC assays. *Molecular and Cellular Biochemistry*, 323(1-2), 139-142. doi:10.1007/s11010-008-9972-5

Botterweck, A., Verhagen, H., Goldbohm, R., Kleinjans, J., & Brandt, P. V. (2000). Intake of butylated hydroxyanisole and butylated hydroxytoluene and stomach cancer risk: Results from

analyses in the Netherlands Cohort Study. *Food and Chemical Toxicology*, 38(7), 599-605. doi:10.1016/s0278-6915(00)00042-9

Canabady-Rochelle, L. L., Harscoat-Schiavo, C., Kessler, V., Aymes, A., Fournier, F., & Girardet, J. (2015). Determination of reducing power and metal chelating ability of antioxidant peptides: Revisited methods. *Food Chemistry*, 183, 129-135. doi:10.1016/j.foodchem.2015.02.147

Huang, D., Ou, B., & Prior, R. L. (2005). The Chemistry behind Antioxidant Capacity Assays. *Journal of Agricultural and Food Chemistry*, 53(6), 1841-1856. doi:10.1021/jf030723c

Huang, W., Seehafer, K., & Bunz, U. H. (2019). Discrimination of Flavonoids by a Hypothesis Free Sensor Array. *ACS Applied Polymer Materials*, 1(6), 1301-1307. doi:10.1021/acsapm.9b00116

Jurs, P. C., Bakken, G. A., & McClelland, H. E. (2000). Computational Methods for the Analysis of Chemical Sensor Array Data from Volatile Analytes. *Chemical Reviews*, 100(7), 2649-2678. doi:10.1021/cr9800964

Ko, J., Bhagwat, N., Yee, S. S., Ortiz, N., Sahnoud, A., Black, T., . . . Issadore, D. (2017). Combining Machine Learning and Nanofluidic Technology To Diagnose Pancreatic Cancer Using Exosomes. *ACS Nano*, 11(11), 11182-11193. doi:10.1021/acsnano.7b05503

Laguette, M., Decker, E. A., Lecomte, J., & Villeneuve, P. (2010). Methods for evaluating the potency and efficacy of antioxidants. *Current Opinion in Clinical Nutrition and Metabolic Care*, 13(5), 518-525. doi:10.1097/mco.0b013e32833aff12

Leeuw, R. V., Kevers, C., Pincemail, J., Defraigne, J., & Dommes, J. (2014). Antioxidant capacity and phenolic composition of red wines from various grape varieties: Specificity of Pinot Noir. *Journal of Food Composition and Analysis*, 36(1-2), 40-50. doi:10.1016/j.jfca.2014.07.001

Li, H., Lin, H., Wang, X., Lv, W., & Li, F. (2019). Dopamine-Based Paper Analytical Device for Truly Equipment-Free and Naked-Eye Biosensing Based on the Target-Initiated Catalyzed Oxidation. *ACS Applied Materials & Interfaces*, *11*(40), 36469-36475. doi:10.1021/acsami.9b14859

Ma, Y., Li, W., Cho, E. C., Li, Z., Yu, T., Zeng, J., . . . Xia, Y. (2010). Au@Ag Core-Shell Nanocubes with Finely Tuned and Well-Controlled Sizes, Shell Thicknesses, and Optical Properties. *ACS Nano*, *4*(11), 6725-6734. doi:10.1021/nn102237c

Piyanan, T., Athipornchai, A., Henry, C. S., & Sameenoi, Y. (2018). An Instrument-free Detection of Antioxidant Activity Using Paper-based Analytical Devices Coated with Nanoceria. *Analytical Sciences*, *34*(1), 97-102. doi:10.2116/analsci.34.97

Prior, R. L., Wu, X., & Schaich, K. (2005). Standardized Methods for the Determination of Antioxidant Capacity and Phenolics in Foods and Dietary Supplements. *Journal of Agricultural and Food Chemistry*, *53*(10), 4290-4302. doi:10.1021/jf0502698

Prior, R. L., Wu, X., & Schaich, K. (2005). Standardized Methods for the Determination of Antioxidant Capacity and Phenolics in Foods and Dietary Supplements. *Journal of Agricultural and Food Chemistry*, *53*(10), 4290-4302. doi:10.1021/jf0502698

Rivero-Pérez, M. D., González-Sanjosé, M. L., Ortega-Herás, M., & Muñoz, P. (2008). Antioxidant potential of single-variety red wines aged in the barrel and in the bottle. *Food Chemistry*, *111*(4), 957-964. doi:10.1016/j.foodchem.2008.05.013

You, C., Miranda, O. R., Gider, B., Ghosh, P. S., Kim, I., Erdogan, B., . . . Rotello, V. M. (2007). Detection and identification of proteins using nanoparticle-fluorescent polymer 'chemical nose' sensors. *Nature Nanotechnology*, *2*(5), 318-323. doi:10.1038/nnano.2007.99

Özyürek, M., Güçlü, K., Tütem, E., Başkan, K. S., Erçağ, E., Çelik, S. E., . . . Apak, R. (2011).

A comprehensive review of CUPRAC methodology. *Analytical Methods*, 3(11), 2439.

doi:10.1039/c1ay05320e

2020 S.-T. Yau High School Science Award

Appendix

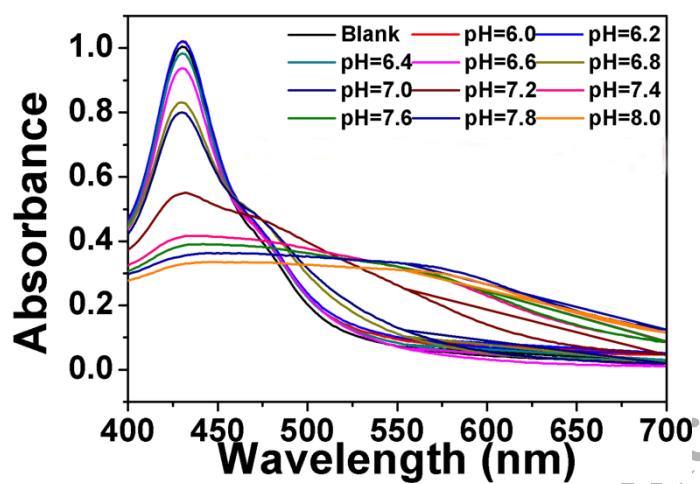


Figure S1 UV-vis spectra of Au@Ag NCs in different pH of solutions in the presence of 40 μM HAuCl_4 and 20 nM AA.

2020 S.-T. Yau High School Science Award

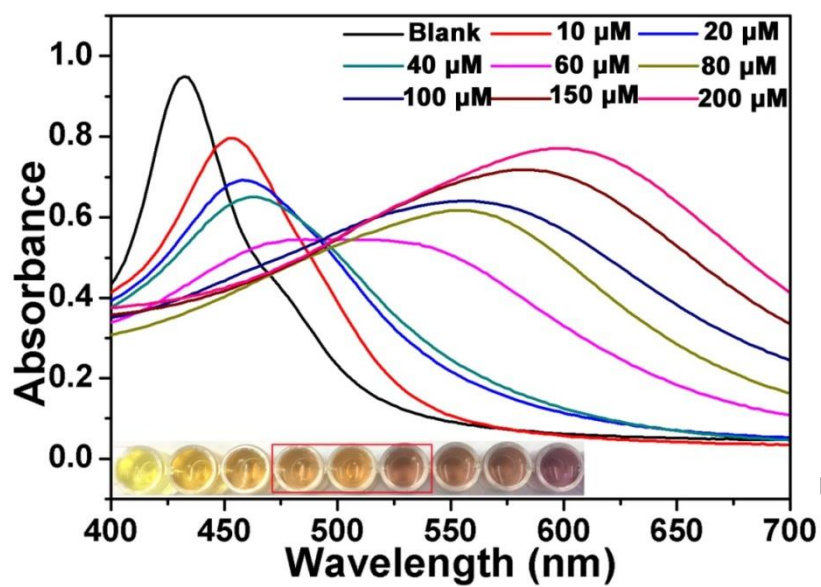


Figure S2 UV-vis spectra of Au@Ag NCs in the presence of different concentrations of HAuCl₄.

2020 S.-T. Yau High School Science Award

Table S1 The training matrix of the colorimetric response patterns against 6 antioxidants by using this sensor assay at the concentration of 200 nM.

Antioxidants	Ai-A0 80 μM Au $^{3+}$	Ai-A0 60 μM Au $^{3+}$	Ai-A0 40 μM Au $^{3+}$
CA	-0.001	0.061	0.013
CA	-0.004	0.063	0.013
CA	-0.003	0.063	0.017
CA	0.001	0.065	0.051
CA	0.003	0.06	0.052
TA	-0.064	0.017	0.116
TA	-0.063	0.017	0.12
TA	-0.06	0.023	0.12
TA	-0.06	0.02	0.155
TA	-0.063	0.017	0.155
AA	0.011	0.045	0.145
AA	0.011	0.044	0.145
AA	0.011	0.049	0.147
AA	0.011	0.047	0.182
AA	0.015	0.048	0.185
TP	-0.039	0.066	0.06
TP	-0.039	0.069	0.063
TP	-0.04	0.072	0.059
TP	-0.04	0.066	0.098
TP	-0.038	0.064	0.1
TCA	-0.098	0.054	0.065
TCA	-0.097	0.056	0.065
TCA	-0.094	0.06	0.063
TCA	-0.096	0.057	0.104
TCA	-0.098	0.053	0.102
GA	0.145	0.068	0.126
GA	0.144	0.07	0.129
GA	0.147	0.074	0.129
GA	0.146	0.069	0.166
GA	0.146	0.066	0.164

Table S2 The training matrix of the colorimetric response patterns against 6 antioxidants by using this sensor assay at the concentration of 150 nM.

Antioxidants	Ai-A0 80 μM Au $^{3+}$	Ai-A0 60 μM Au $^{3+}$	Ai-A0 40 μM Au $^{3+}$
CA	-0.051	0.011	-0.018
CA	-0.052	0.011	-0.017
CA	-0.051	0.011	-0.017
CA	-0.052	0.013	-0.017
CA	-0.052	0.01	-0.02
TA	-0.074	-0.051	-0.065
TA	-0.074	-0.051	-0.065
TA	-0.074	-0.048	-0.064
TA	-0.076	-0.048	-0.063
TA	-0.075	-0.051	-0.065
AA	-0.176	-0.133	-0.038
AA	-0.174	-0.131	-0.038
AA	-0.176	-0.129	-0.04
AA	-0.177	-0.131	-0.034
AA	-0.177	-0.134	-0.04
TP	-0.054	-0.052	-0.055
TP	-0.052	-0.05	-0.053
TP	-0.056	-0.051	-0.056
TP	-0.054	-0.049	-0.051
TP	-0.052	-0.054	-0.055
TCA	-0.055	-0.105	-0.032
TCA	-0.053	-0.102	-0.03
TCA	-0.054	-0.102	-0.03
TCA	-0.056	-0.105	-0.027
TCA	-0.056	-0.105	-0.032
GA	-0.046	-0.093	-0.117
GA	-0.047	-0.091	-0.115
GA	-0.048	-0.09	-0.115
GA	-0.045	-0.097	-0.114
GA	-0.045	-0.095	-0.115

Table S3 The training matrix of the colorimetric response patterns against 6 antioxidants by using this sensor assay at the concentration of 100 nM.

Antioxidants	Ai-A0 80 μM Au $^{3+}$	Ai-A0 60 μM Au $^{3+}$	Ai-A0 40 μM Au $^{3+}$
CA	-0.044	0.028	0.158
CA	-0.049	0.026	0.162
CA	-0.043	0.028	0.169
CA	-0.045	0.029	0.166
CA	-0.041	0.028	0.16
TA	-0.063	-0.102	0.074
TA	-0.061	-0.099	0.079
TA	-0.058	-0.094	0.076
TA	-0.063	-0.101	0.078
TA	-0.061	-0.108	0.07
AA	-0.084	0.06	0.125
AA	-0.084	0.065	0.126
AA	-0.087	0.067	0.132
AA	-0.084	0.059	0.124
AA	-0.085	0.053	0.123
TP	-0.035	0.072	-0.02
TP	-0.035	0.069	-0.02
TP	-0.032	0.078	-0.013
TP	-0.029	0.07	-0.01
TP	-0.037	0.067	-0.022
TCA	-0.132	-0.006	0.06
TCA	-0.137	-0.001	0.058
TCA	-0.134	-0.007	0.067
TCA	-0.127	-0.007	0.071
TCA	-0.132	-0.014	0.058
GA	-0.115	0.022	0.033
GA	-0.119	0.024	0.039
GA	-0.112	0.02	0.03
GA	-0.109	0.023	0.034
GA	-0.112	0.017	0.036

Table S4 The training matrix of the colorimetric response patterns against 6 antioxidants by using this sensor assay at the concentration of 50 nM.

Antioxidants	Ai-A0 80 μM Au $^{3+}$	Ai-A0 60 μM Au $^{3+}$	Ai-A0 40 μM Au $^{3+}$
CA	0.021	0.036	-0.021
CA	0.02	0.034	-0.022
CA	0.017	0.032	-0.023
CA	0.023	0.032	-0.019
CA	0.026	0.032	-0.02
TA	0.008	0.042	0.015
TA	0.007	0.042	0.011
TA	0.006	0.038	0.013
TA	0.01	0.04	0.02
TA	0.013	0.039	0.016
AA	0.034	0.049	-0.077
AA	0.033	0.046	-0.081
AA	0.03	0.05	-0.077
AA	0.033	0.052	-0.071
AA	0.038	0.046	-0.074
TP	-0.015	0.043	-0.018
TP	-0.012	0.045	-0.022
TP	-0.017	0.038	-0.022
TP	-0.014	0.047	-0.011
TP	-0.012	0.039	-0.015
TCA	-0.003	0.024	-0.031
TCA	-0.003	0.024	-0.034
TCA	-0.005	0.025	-0.032
TCA	-0.003	0.024	-0.029
TCA	-0.003	0.019	-0.029
GA	0.009	0.064	-0.027
GA	0.011	0.064	-0.027
GA	0.008	0.059	-0.027
GA	0.01	0.065	-0.023
GA	0.009	0.062	-0.023

Table S5 The training matrix of the colorimetric response patterns against 6 antioxidants by using this sensor assay at the concentration of 20 nM.

Antioxidants	Ai-A0 80 μM Au $^{3+}$	Ai-A0 60 μM Au $^{3+}$	Ai-A0 40 μM Au $^{3+}$
CA	-0.008	0.007	-0.01
CA	-0.013	0.007	-0.015
CA	-0.009	0.004	-0.013
CA	-0.011	0.008	-0.014
CA	-0.008	0.004	-0.009
TA	0.046	-0.021	-0.046
TA	0.045	-0.022	-0.047
TA	0.044	-0.022	-0.048
TA	0.045	-0.021	-0.048
TA	0.045	-0.026	-0.044
AA	0.033	0.042	0.03
AA	0.032	0.043	0.03
AA	0.03	0.043	0.032
AA	0.03	0.039	0.027
AA	0.034	0.04	0.03
TP	0.014	0.026	-0.005
TP	-0.003	0.028	-0.009
TP	0.011	0.025	-0.005
TP	0.011	0.025	-0.011
TP	0.014	0.019	-0.006
TCA	-0.003	0.102	0.032
TCA	-0.005	0.104	0.029
TCA	-0.005	0.103	0.029
TCA	-0.004	0.101	0.03
TCA	-0.004	0.096	0.033
GA	0.014	0.02	0.078
GA	0.012	0.023	0.075
GA	0.016	0.018	0.075
GA	0.012	0.018	0.077
GA	0.012	0.018	0.082

Table S6 The training matrix of the colorimetric response patterns against 6 antioxidants by using this sensor assay at the concentration of 10 nM.ice

Antioxidants	Ai-A0 80 $\mu\text{M Au}^{3+}$	Ai-A0 60 $\mu\text{M Au}^{3+}$	Ai-A0 40 $\mu\text{M Au}^{3+}$
CA	0.095	0.016	-0.051
CA	0.094	0.016	-0.049
CA	0.094	0.014	-0.05
CA	0.094	0.019	-0.057
CA	0.093	0.018	-0.05
TA	0.074	0.005	-0.004
TA	0.075	0.005	0.001
TA	0.076	0.003	0
TA	0.072	0.002	-0.009
TA	0.074	0.011	-0.006
AA	0.16	0.022	0.022
AA	0.163	0.027	0.026
AA	0.165	0.028	0.024
AA	0.159	0.026	0.02
AA	0.16	0.028	0.02
TP	0.094	0.017	-0.003
TP	0.095	0.017	0.001
TP	0.097	0.015	0.003
TP	0.09	0.019	-0.007
TP	0.093	0.019	-0.002
TCA	0.05	0.054	-0.027
TCA	0.048	0.055	-0.024
TCA	0.05	0.056	-0.024
TCA	0.051	0.058	-0.032
TCA	0.052	0.059	-0.031
GA	0.097	0.05	-0.05
GA	0.1	0.053	-0.049
GA	0.099	0.054	-0.045
GA	0.094	0.048	-0.05
GA	0.094	0.052	-0.053

Table S7 The training matrix of the colorimetric response patterns against the mixture of 2/3/4/5 and 6 kinds of antioxidants at 100 nM by using this sensor assay.

Antioxidants	Ai-A0 80 μM Au ³⁺	Ai-A0 60 μM Au ³⁺	Ai-A0 40 μM Au ³⁺
CA:TA=4:6	0.131	0.001	0.038
CA:TA=4:6	0.129	0	0.039
CA:TA=4:6	0.13	0.004	0.04
CA:TA=4:6	0.13	0.002	0.038
CA:TA=4:6	0.133	0.001	0.037
AA:TP:TCA=3:3:4	0.025	-0.032	-0.011
AA:TP:TCA=3:3:4	0.022	-0.032	-0.012
AA:TP:TCA=3:3:4	0.022	-0.027	-0.01
AA:TP:TCA=3:3:4	0.021	-0.029	-0.011
AA:TP:TCA=3:3:4	0.025	-0.034	-0.015
CA:TA:GA=4:3:3	0.039	0.01	0.033
CA:TA:GA=4:3:3	0.039	0.01	0.034
CA:TA:GA=4:3:3	0.035	0.014	0.032
CA:TA:GA=4:3:3	0.04	0.01	0.036
CA:TA:GA=4:3:3	0.043	0.011	0.032
CA:AA:TP:TCA=1:2: 3:4	0.067	-0.047	0.064
CA:AA:TP:TCA=1:2: 3:4	0.067	-0.047	0.068
CA:AA:TP:TCA=1:2: 3:4	0.062	-0.042	0.065
CA:AA:TP:TCA=1:2: 3:4	0.066	-0.045	0.064
CA:AA:TP:TCA=1:2: 3:4	0.067	-0.047	0.063
CA:TA:TP:TCA:GA= 2:1:2:3:2	0.071	-0.018	0.046
CA:TA:TP:TCA:GA= 2:1:2:3:2	0.069	-0.016	0.05
CA:TA:TP:TCA:GA= 2:1:2:3:2	0.07	-0.012	0.049
CA:TA:TP:TCA:GA= 2:1:2:3:2	0.071	-0.015	0.047
CA:TA:TP:TCA:GA= 2:1:2:3:2	0.075	-0.017	0.045
CA:TA:AA:TP:TCA: GA=2:2:1:2:1:2	0.05	0.011	0.019
CA:TA:AA:TP:TCA: GA=2:2:1:2:1:2	0.047	0.009	0.023
CA:TA:AA:TP:TCA: GA=2:2:1:2:1:2	0.044	0.012	0.022
CA:TA:AA:TP:TCA: GA=2:2:1:2:1:2	0.051	0.011	0.019

CA:TA:AA:TP:TCA: GA=2:2:1:2:1:2	0.052	0.009	0.015
------------------------------------	-------	-------	-------

2020 S.-T. Yau High School Science Award

Table S8 The training matrix of the colorimetric response patterns against the 6 antioxidants at 20 nM in urine samples by using this sensor assay.

Antioxidants	$A_i - A_0$ 80 $\mu\text{M Au}^{3+}$	$A_i - A_0$ 60 $\mu\text{M Au}^{3+}$	$A_i - A_0$ 40 $\mu\text{M Au}^{3+}$
Serum	0.02	-0.02	-0.039
Serum	-0.001	-0.024	-0.04
Serum	0.021	-0.022	-0.04
Serum	0.017	-0.019	-0.037
Serum	0.022	-0.022	-0.038
CA	0.072	0.019	-0.05
CA	0.075	0.015	-0.05
CA	0.07	0.016	-0.052
CA	0.069	0.02	-0.048
CA	0.071	0.018	-0.053
TA	0.118	-0.052	-0.037
TA	0.119	-0.053	-0.037
TA	0.121	-0.05	-0.04
TA	0.117	-0.05	-0.037
TA	0.121	-0.052	-0.037
AA	0.073	0.043	-0.045
AA	0.074	0.038	-0.036
AA	0.075	0.043	-0.048
AA	0.069	0.044	-0.046
AA	0.073	0.04	-0.047
TP	0.079	0.031	-0.108
TP	0.08	0.027	-0.111
TP	0.081	0.032	-0.107
TP	0.077	0.033	-0.105
TP	0.082	0.028	-0.111
TCA	0.124	-0.057	-0.008
TCA	0.124	-0.058	-0.011
TCA	0.126	-0.056	-0.007
TCA	0.121	-0.055	-0.008
TCA	0.123	-0.059	-0.011
GA	-0.037	-0.001	-0.074
GA	-0.036	-0.002	-0.073
GA	-0.035	0.001	-0.074
GA	-0.04	0	-0.071
GA	-0.034	-0.002	-0.076